Shear Interaction of High-Strength Two-Layered Concretes at Early Ages Placed in Subfreezing Temperatures

SHIVAPRASAD T. KUDLAPUR AND EDWARD G. NAWY

There are few studies on the early-age performance of high-strength cold weather concretes and their shear strength interaction in cold weather. Shear strength characteristics of high-strength cold weather concrete in subfreezing temperatures is the topic of this paper. Tests were conducted on cylinders and L-shaped push-off specimens to determine the early-age shear interlock and shear frictional resistance between high-strength regular portland cement concrete and cold weather high-strength concretes in the rehabilitation of bridge decks and other infrastructure systems. Results validate previous findings on polymer-modified concretes: the American Concrete Institute code limits on the shear-friction strength are too conservative even at early ages of high-strength cold weather concretes and need to be modified.

Previous investigations have identified materials and methods to repair concrete bridges in subfreezing winter conditions (*1*,*2*). A preliminary screening phase was performed to select potentially suitable materials from among 17 materials identified by a literature survey (Phase I). On the basis of Phase I results, five products representing four generically distinct materials were selected for further investigation. The selected materials were two methylmethacrylate (MMA)-based polymer concretes, one water-based and one non-water-based magnesium phosphate concrete, and one polyurethane-based polymer concrete. These materials were studied in depth in Phase II, which included cylinder compressive strength tests, cylinder shear bond strength tests, static and cyclic flexural tests of patched prism specimens, corrosion and durability tests of patched prism specimens, and static and cyclic flexural tests of patched slab specimens.

PERFORMANCE TESTING

Cylinder Tests

Three cylinders of each specimen type were tested in compression for compressive and slant shear strengths at 24 hr and 7 days after casting, and curing in the cold room for the full period. Two sets of cylinders were cast out of each of the two MMA-based materials—one with and one without gravel. Results of the cylinder compressive strengths are shown in Figure 1. It can be observed that all materials possess strength at early age. Gain in strength for the MMA samples containing stone, M1(G) and M2(G), at 24 hr is about 86 percent of their final strength, whereas this value is about 91 percent for magnesium phosphate concrete. MMA mixes behave differently with and without stone. Whereas MMA mixes with stone increase in strength with age, the neat MMA mixes (without stone) decrease with age. The reduction of strength with age of MMA without stone can be attributed to microcracking caused by differential shrinkage. The slant shear strengths for dry-patched and moist-patched specimens are presented in Figure 2. These results provide a comparative measure of shear bond. They also indicate that all the materials possess a reasonable amount of good bond strength at an early age. The reduction of strength with age of MMA materials without stone is again apparent. Gravel-containing MMA concrete shows a gain of only 5.23 percent of bond strength after 24 hr, whereas magnesium phosphate concrete exhibits about 47 percent gain in bond strength.

Rutgers University—The State University of New Jersey, P.O. Box 909, Piscataway, N.J. 08855. *Current affiliation:* S. T. Kudlapur, Jablonski & Mead Associates, 1200 MacArthur Blvd., Mahwah, N.J. 07430.

Flexure Tests

Prism specimens for flexure tests (both static and fatigue) were patched in the cold room with patching materials prepared according to manufacturers' instructions. The patch surfaces were as formed and untreated. Specimens were tested at 7 days of age. Three patch depths were used to assess the effect of patch boundary on the response: shallow, half depth, and full depth. The shallow patches (depth 0.5 in.) with MMA materials did not contain stone but other depths contained ⅜ in. stone. Results of flexure tests indicated that the flexural strengths of the patched specimens were comparable with those of the control specimens.

Freeze-Thaw Tests

Durability tests were performed on patched prism specimens by subjecting them to 300 freeze-thaw cycles (ASTM C 666, Procedure A). Three patch depths were tested. Weight and half-cell potential were measured before cycling and at intervals not greater than 36 cycles. Half-cell readings were taken adjacent to each patch boundary. The results indicated that all materials other than water-based magnesium phosphate showed better freeze-thaw durability than the parent concrete. Observations on the corrosion of reinforcement in freeze-thaw specimens following break-up of specimens indicated substantial corrosion at the patch boundaries of all materials tested.

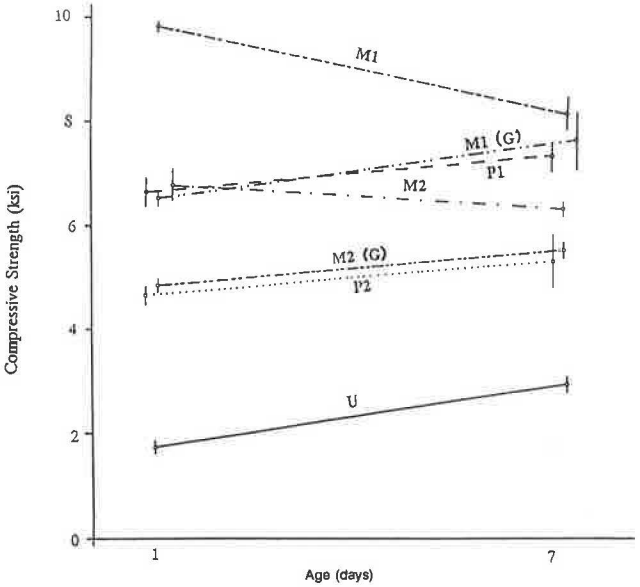

M1, M2--MMA-based polymer concretes
M1(G), M2(G)--MMA-based polymer concretes with 3/8 in. gravel satisfying ASTM C 33 (pea gravel)
P1, P2--water and non-water-based magnesium phosphate concretes
U--Polyurethane polymer concrete

FIGURE 1 Cylinder compressive strength test results.

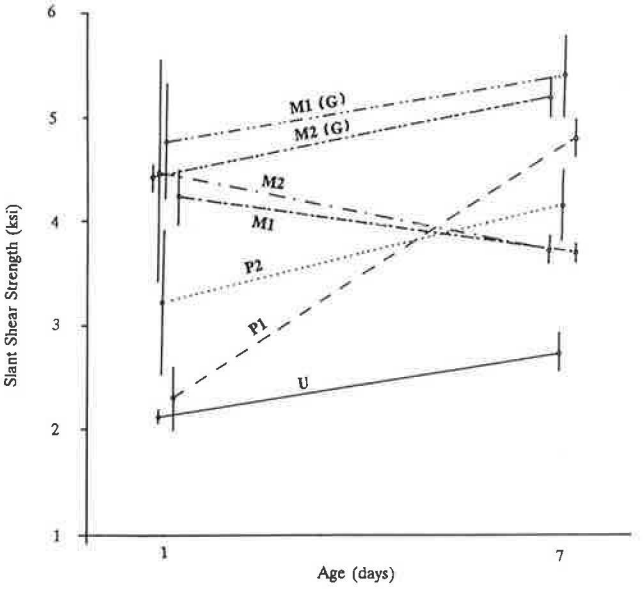

(a) Dry Patched Specimens

M1, M2--MMA-based polymer concrete
M1(G), M2(G)--MMA-based polymer concrete with 3/8 in. pea gravel satisfying ASTM C33
P1, P2--Water and non-water-based magnesium phosphate concretes
U--Polyurethane polymer concrete

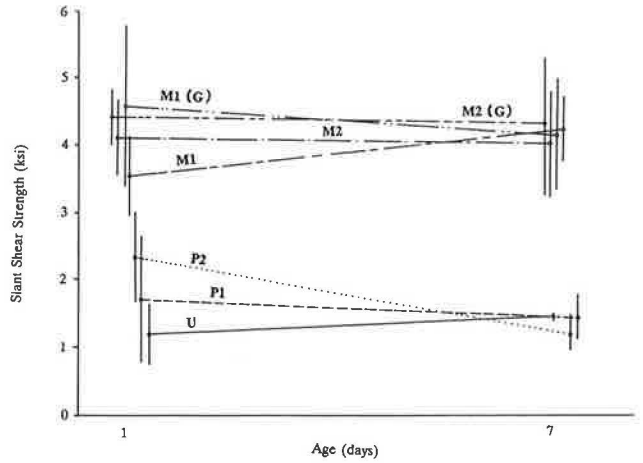

(b) Moist Patched Specimens

M1, M2--MMA-based polymer concrete
M1(G), M2(G)--MMA-based polymer concrete with 3/8 in. pea gravel satisfying ASTM C33
P1, P2--Water and non-water-based magnesium phosphate concretes
U--Polyurethane polymer concrete

FIGURE 2 Cylinder slant shear strength test results.

Summary

The program consisted of a series of factorial experiments. The factors tested were material type, age, and repair depth. The effects of these factors were assessed with an analysis of variance. MMA-based materials and magnesium phosphate-based materials were thus identified as performing satisfactorily at subfreezing temperatures. The MMA-based materials exhibited superior performance over the magnesium phosphate-based materials, particularly on measures of freeze-thaw performance. As far as handling is concerned, magnesium phosphate-based materials showed distinct advantages over the volatile and odorous MMA-based materials.

PRESENT INVESTIGATION

This study concerns the shear transfer mechanism of cold weather repair materials, specifically, the conditions under which failure of interacting bonded surfaces takes place between precast and cast in situ elements in buildings and concrete bridges and in patched sections in bridge deck slabs. Examples are the interface between a precast beam and a cast-in-place floor slab or a vertical plane at the upper reentrant corner of a corbel when repair is necessary under subfreezing conditions. Suitable materials with their shear transfer performance characteristics are needed to repair the damaged structural components. Prediction and knowledge of early-age shear strength at subfreezing temperatures are essential if concrete has to be installed in cold weather.

Current literature describes the shear friction mechanism and dowel action of initially cracked or uncracked regular concrete (*3–8*) or epoxy-modified polymer concrete (*9–11*) bonded to regular concrete surfaces. This investigation was designed to assess the applicability of these results to cold weather repair materials cast at cold temperatures. The two MMA concretes discussed at the beginning of this paper were selected for study on the basis of their overall satisfactory performance. This paper focuses on shear transfer of regular high-strength concrete with (a) MMA-based polymer concrete and (b) magnesium phosphate-based concrete at cold temperatures. The load-deformation behavior of these materials under shearing loads is presented and analyzed.

The main objectives of this investigation were to

1. Determine the early-age shear strength characteristics and shear transfer properties of the MMA polymer concrete and magnesium phosphate concretes cast at subfreezing temperatures at their interaction surface with the parent concrete;

2. Verify the applicability of the "shear friction theory" to the calculation of the direct shear strength using these two repair materials;
3. Evaluate the necessary constants of the theoretical expressions; and
4. Check the validity of the American Concrete Institute (ACI) code limits for high-strength cold weather concretes.

EXPERIMENTAL INVESTIGATION OF THE SHEAR TRANSFER MECHANISM

Materials, Mix Proportion, and Fabrication

Typical test specimens are shown in Figure 3. The shape and size of these specimens were chosen on the basis of successful results obtained for epoxy-modified polymer concrete (*9–11*). When such specimens are loaded axially, shear is produced on the shear plane. By providing adequate longitudinal and end reinforcement, it is assumed that only a negligible moment is produced on the shear plane and that the specimen would fail in shear along the shear plane. The end reinforcement also prevents the top and bottom heads from failing. Actually, the top and bottom heads are elastic in nature. Hence, the loads applied induce flexural stresses of small magnitudes in cold jointed surfaces. If horizontal clamps are used to prevent this rotation, unmeasurable but significant compressive stresses will be induced in the specimen. Thus this was not done. It was therefore assumed that these flexural stresses are negligible in cold jointed surfaces and that the specimen is subjected to pure shear failure. In practice, there is no one test set-up that produces pure shear failure.

In this study, the shear reinforcing strength was varied for both the bar size and the spacing. The bar sizes used were either W4.5 high-strength wire of diameter 0.24 in. or No. 3, as shown in Figure 3. One series of specimens with no transverse reinforcement and three series with transverse shear reinforcement were tested. These are termed specimens with no transverse reinforcement, with light, medium or moderate, and heavy transverse reinforcement, respectively, with vary-

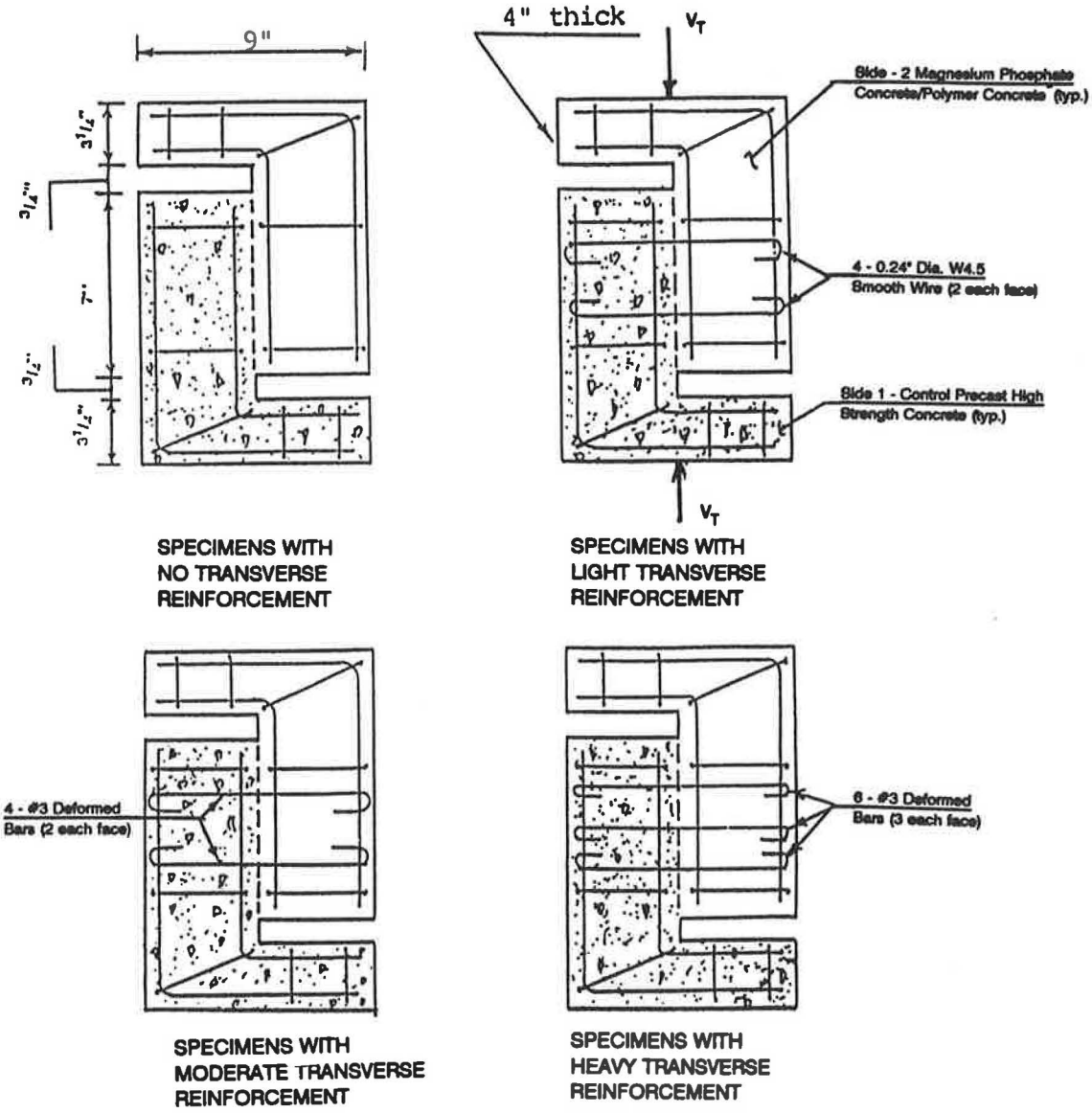

FIGURE 3 Push-off shear test specimens.

ing magnitude of reinforcing steel. "Light," "moderate or medium," and "heavy" are used to indicate different degrees of reinforcement only. The transverse reinforcement crossed the shear plane at 90 degrees. The bar spacings are not shown because they do not have any effect on the shear transfer strength (*7*).

A high-strength concrete mix developed at Rutgers University civil engineering laboratory was used for the control and precast half of the test specimens. This concrete was made from Type III portland cement, ⅜-in. maximum size coarse aggregate, and natural river sand with a fineness modulus of 2.61 for the fine aggregate. The coarse aggregate was washed before use and sand was used in its natural, partially presoaked condition with appropriate allowances for the absorption characteristics. Microsilica, superplasticizer, and a low water-to-cement ratio were used to obtain a high-strength concrete. All test specimens and cylinders were air cured for 24 hr in the mold under polyethylene sheets and then stored in the moisture curing room. The 4- × 8-in. cylinders were tested at 28 days and yielded compressive strengths of 12,000 to 14,500 psi. The test specimens were cured for 30 days before the other half was cast. The second half of the specimens was cast with magnesium phosphate and MMA polymer concrete, following the manufacturers' instructions, in the cold room at a temperature of 15° to 20°F. These were tested at 1, 3, and 7 days of age. The control specimens were included for comparison of shear behavior of cold concretes cast with precast regular concretes.

Instrumentation and Testing of Specimens

In all the specimens reinforced with transverse bars, the steel strains were measured by electric strain gauges mounted a small distance away from the shear plane. Two strain gauges were used for specimens with light and moderate transverse reinforcement, whereas the heavily reinforced specimens carried three gauges on three of the six transverse bars. The vertical slip and the horizontal crack width were measured by linear variable differential transformers (LVDTs) mounted on the specimens as shown in Figure 4 and connected to a Hewlett Packard data acquisition computer system. All the specimens were tested by using a compression testing machine (Figure 5).

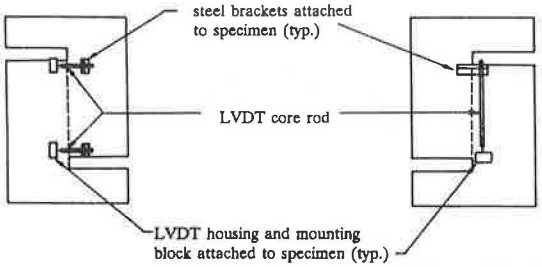

(i) Crack width measurement instrumentation (rear face) (ii) Vertical slip measurement instrumentation (front face)

FIGURE 4 Instrumentation details.

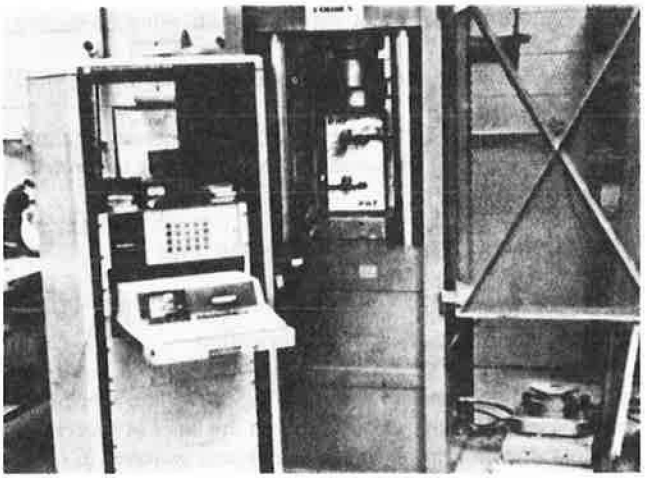

FIGURE 5 Test setup.

SHEAR TRANSFER MECHANISM THEORY FOR CONCRETE

A concrete element offers four types of shear resistance for shear transfer capacity (*11*): intrinsic bond shear resistance V_b (*12*), shear friction resistance V_f (*3,5–7,13*), aggregate interlock mechanism V_i (*8,14*), and dowel action resistance V_d (*15*).

Figure 6 shows a concrete element subjected to a shearing load and Figure 7 shows the dowel shear transfer test config-

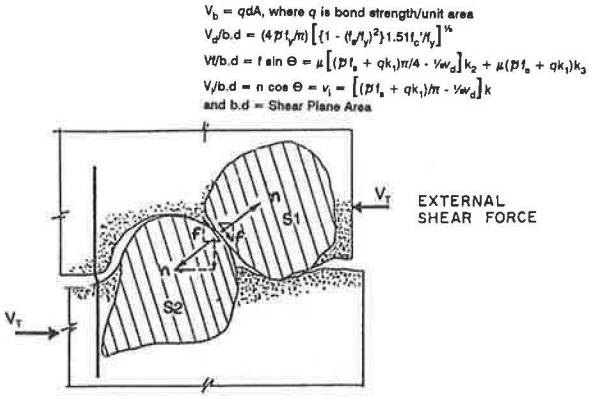

(i) Aggregate Interlock Forces

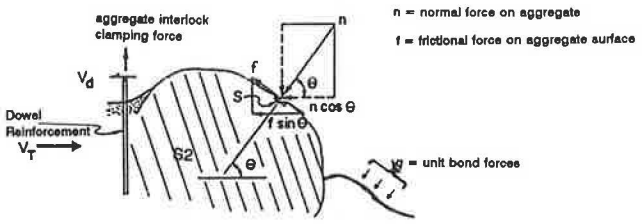

(ii) Force Components

FIGURE 6 Idealized element in shear resistance through friction ($f \sin \theta$), aggregate interlock ($n \cos \theta$), and dowel action (V_d).

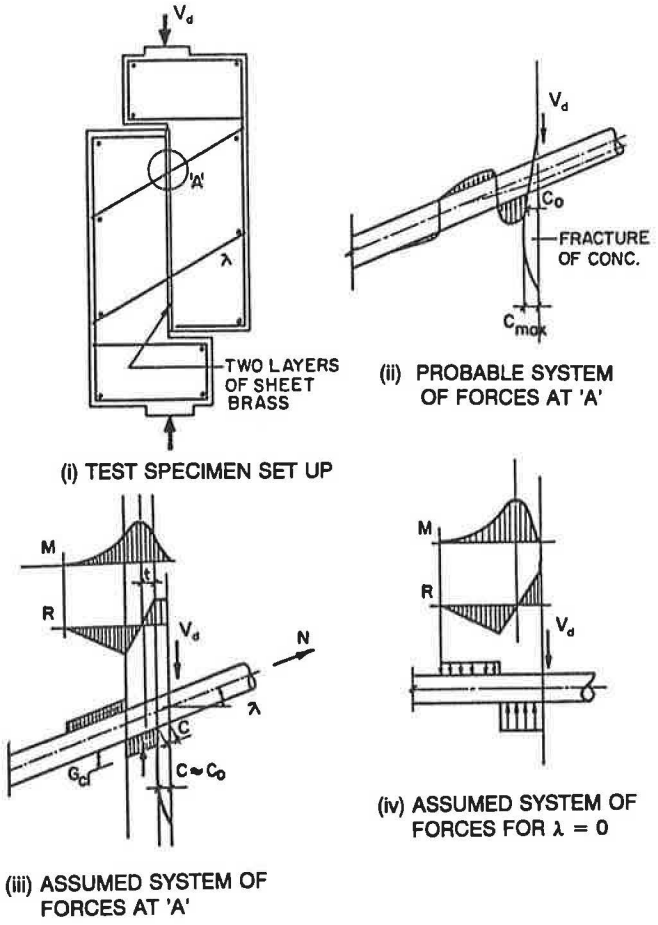

FIGURE 7 System of forces and test configuration for the evaluation of dowel shear transfer strength, *I* (*15*).

uration for evaluating V_d (*15*). Under these loading conditions, initial resistance is offered by the intrinsic bond. When the element cracks, slipping takes place along the shear plane and the shear plane faces are forced to separate. The relative displacement of the concrete on the two sides of the plane produces strains in the reinforcement crossing the shear plane. The result of the forces induced in the reinforcement will have a component parallel to the plane resisting the applied shear and a component normal to the plane that produces a compressive force across the plane. This compressive force produces a frictional resistance to sliding between the faces of the plane, thus opposing the applied shear. The relative movement of the concrete on opposite sides of the plane also subjects the reinforcing steel to a shearing action. The resistance of the reinforcing steel to this shearing action is called dowel action and also contributes to the shearing resistance. Further resistance is provided by aggregate interlock resulting from the interlocking action of the aggregates at the failure plane. Summing up the components of these forces in the horizontal direction yields

$$V_t = V_b + V_f + V_d + V_i \tag{1}$$

Bond shear strength is an intrinsic property of a given concrete mass or epoxy polymer-modified concrete (*9*,*15*). Extending the analogy to MMA polymer concrete and magnesium phosphate concrete, the bond shear resistance can be represented as $V_b = qdA$, where q is the strength per unit bond area. If the ratio of the bond area to the total shear area is k_1, the average bond shear strength is given by

$$v_b = qk_1 \tag{2}$$

Dulacska (*15*) has developed an expression for the load that is transferred by dowel action and is given as

$$V_d = \zeta d_b^2 \Gamma f_y \cdot C \sin\lambda \{(1 + \sigma_c/(3\zeta\omega^2 f_y C \sin^2\lambda))^{1/2} - 1\} \tag{3}$$

where

V_d = shear force transferred by dowel action,
ζ = dowel resistance ratio = $\{1 - (N/N_y)^2\}$ = $\{1 - (f_s/f_y)^2\}$,
N = tensile force in the dowel bar = $A_s f_s$,
N_y = tensile yield force = $A_s f_y$,
d_b = diameter of transverse bar,
ω = constant (0.05),
f_y = steel yield stress,
C = coefficient of local compression of concrete = 4,
λ = angle between transverse bar and the perpendicular to the shear plane (Figure 5b), and
σ_c = cube strength of concrete ($= 1.13\, f'_c$).

Rearranging the terms in the above expression gives

$$V_d = \{(\zeta d_b^2 \omega f_y C \sin\lambda)^2 + [\sigma_c(\zeta d_b^2 \omega f_y C \sin\lambda)^2]/[3\zeta\omega^2 f_y C \sin^2\lambda]\} - \zeta d_b^2 \omega \sin\lambda \tag{4}$$

If a transverse bar crosses the shear plane at 90 degrees, $\lambda = 0 \rightarrow \sin\lambda = 0$

$$V_d = (\zeta d_b^4 f_y C \sigma_c/3)^{1/2} = d_b^2 (\zeta f_y C \sigma_c/3)^{1/2} \tag{5}$$

If n is the number of transverse bars crossing the shear plane with diameter d_b and $d_b^2 = 4A_s/\pi$, substituting for the known terms from above, the total shear force becomes

$$nV_d = (4nA_s/\pi)\,[\{1 - (f_s/f_y)^2\}1.51 f'_c f_y/3]^{1/2} \tag{6}$$

Shear stress over the cross section area bd is given by

$$v_d = nV_d/bd$$

If shear reinforcement ratio is denoted by $\bar{\rho}$, which is equal to nA_s/bd, then dowel action shear resistance is

$$v_d = (4\bar{\rho} f_y/\pi)\,[\{1 - (f_s/f_y)^2\}1.51 f'_c/f_y]^{1/2} \tag{7}$$

Shear resistance due to frictional force (*9–11*) is given by

$$v_f = \mu[(\bar{\rho}f_s + qk_1)\pi/4 - {}^1/_2 v_d]k_2 + \mu(\bar{\rho}f_s + qk_1)k_3 \quad (8)$$

and shear resistance due to aggregate interlock (*9–11*) is given by

$$v_i = [(\bar{\rho}f_s + qk_1)/\pi - {}^1/_2 v_d]k_2 \quad (9)$$

where

μ = coefficient of friction,
k_1 = ratio of bond area to total shear area,
k_2 = ratio of projected area of aggregate to the total shear plane cross-sectional area,
k_3 = ratio of the area unoccupied by the aggregates to that of the total shear at the shear plane $\approx 1 - k_1 - k_2$, and
q = bond shear strength per unit area.

Adding all the components of shear resistance and rearranging terms yields

$$v_t = qk_1 + (4\bar{\rho}f_y/\pi)[\{1 - (f_s/f_y)^2\}1.51f'_c/f_y]^{1/2}[1 - (k_2/2)(1 + \mu)] + (\bar{\rho}f_s + qk_1)\{\mu k_3 + k_2\pi(\mu/4 + 1/\pi^2)\} \quad (10)$$

In this expression, the constant terms ½, $\pi/4$, π, and so on are known to represent the shape of the aggregates in the concrete matrix.

Members with No Shear Transfer Reinforcement

Substituting $\bar{\rho} = 0$ in the expression for total shear resistance, Equation 10 reduces to

$$v_t = qk_1 + qk_1[\mu k_3 + k_2\pi(\mu/4 + 1/\pi^2)] = \text{a constant} \quad (11)$$

Because every term in this expression is a constant for a given surface, v_t is a constant and is termed the "apparent cohesive strength" and is nothing but the bond strength of the materials. In regular concrete and magnesium phosphate concrete joints this magnitude of shear resistance is small and is consistent with the test results. But in polymer concrete, because MMA is a liquid with low viscosity, it flows freely into all the microcracks and forms a polymer matrix by bridging all the cracks. This action induces compressive stress against the plane and helps in the development of additional shear strength through friction and aggregate interlock mechanisms and hence a higher total shear strength for MMA concrete.

Members with Transverse Shear Reinforcement

When specimens with transverse reinforcement are subjected to shear along the shear plane, slipping takes place, thereby inducing stresses in the transverse steel. This transverse steel has been found to develop its yield strength at ultimate as indicated by the readings of the electric strain gauges at the onset of ultimate stress. It is therefore reasonable to assume that at ultimate loads, the strain in reinforcement normal to the shear plane is equal to its yield strain and, hence, the stress is equal to the yield stress. Substituting f_y for f_s in the expression for v_t in Equation 10

$$v_t = (qk_1) + (\bar{\rho}f_y + qk_1)\{\mu k_3 + k_2\pi(\mu/4 + 1/\pi^2)\} \quad (12)$$

Grouping the constant terms will yield

$$v_t = \bar{\rho}f_y\{\mu k_3 + k_2\pi(\mu/4 + 1/\pi^2)\} + qk_1\{1 + \mu k_3 + k_2\pi(\mu/4 + 1/\pi^2)\} \quad (13)$$

$$v_t = \bar{\rho}f_y\mu' + c' \quad (14)$$

where

$\mu' = \{\mu k_3 + k_2\pi(\mu/4 + 1/\pi^2)\}$
$c' = (qk_1)(1 + \mu')$

Let I be the shear reinforcing index $= \bar{\rho}f_y$. Then

$$v_t = I\mu' + c' \quad (15)$$

In Equation 15, c' is the apparent cohesion: the shear resistance resulting from bond action, which is the same as the shear strength for cases with no shear reinforcement. The term μ' is called the apparent coefficient of friction and combines the effect of friction with aggregate interlock actions. Equation 15 is similar to those developed by Hermanson and Cowan (*16*) and ACI (*17*) given by $v_t = I\mu$. Hermanson and ACI apparently did not account for the shear bond strength. Equation 15 is the same as the equations Ukadike (*11*) and Nawy (*9,10*) developed for moderate reinforcement by neglecting the dowel action, assuming that its contribution is negligible after the yielding of transverse steel. By the strain gauge results, transverse steel reached its yield at the onset of ultimate and were stressed beyond their yield values in most of the specimens. This yielding of transverse steel is caused by the separation of the shear plane faces. Therefore, at ultimate strength, the compressive force across the crack after the separation of the shear plane faces is just the yield force in the reinforcement. The frictional resistance to shear along the crack is then equal to this force multiplied by the coefficient of friction of the concrete. The apparent coefficient of friction, μ' in Equation 15, therefore, includes this frictional shear resistance in addition to dowel action and aggregate interlock shear resistances.

DISCUSSION OF RESULTS

Behavior of Test Specimens Under the Action of Shear Loads

Specimens with no transverse reinforcement for both the magnesium phosphate and the polymer concretes exhibited similar modes of failure of vertical slippage along the shear plane. Specimens with light reinforcement experienced rupture of one to two steel bars at and beyond yield loads. Moderately and heavily reinforced specimens, on the other hand, failed

in a ductile manner at strain levels greater than their yield strains and while in the strain hardening stage. Neither vertical cracks nor spalls were noticed for either of the two nonreinforced and lightly reinforced concrete specimens (Figure 8). Although the moderate and heavily reinforced magnesium phosphate concrete specimens showed material spalls on the cast-in-place half at ultimate loading conditions, the similarly reinforced polymer concrete specimens exhibited regular concrete spalls (Figures 9 and 10). No noticeable difference in test specimen behavior was observed at different ages for the same material and reinforcement.

Effect of Age

Effect of age on shear transfer strength is presented in Figure 11 for magnesium phosphate and polymer concretes with various levels of reinforcement. Most of the shear transfer strength of the magnesium phosphate concrete, with or without reinforcement, is attained at 24 hr; further gain in strength is insignificant thereafter. In contrast, MMA polymer concrete specimens of similar geometry show some gain in shear transfer strength between 24 hr and 7 days. As the amount of shear reinforcement increases, a gradual gain in shear transfer strength

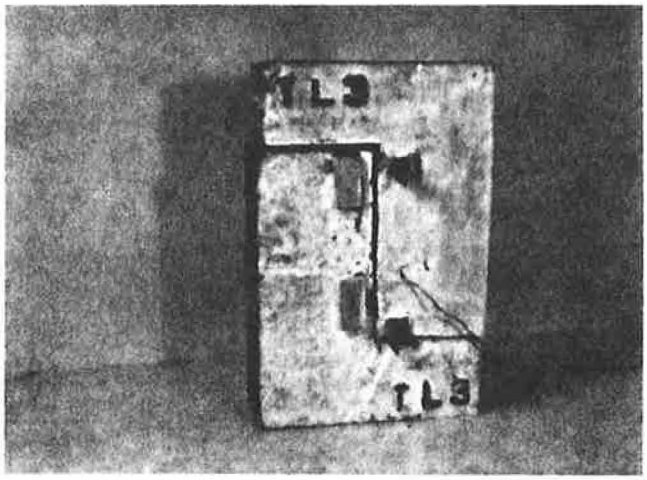

FIGURE 8 Typical failure of TN, TL, PN, and PL specimens (slippage along the shear plane).

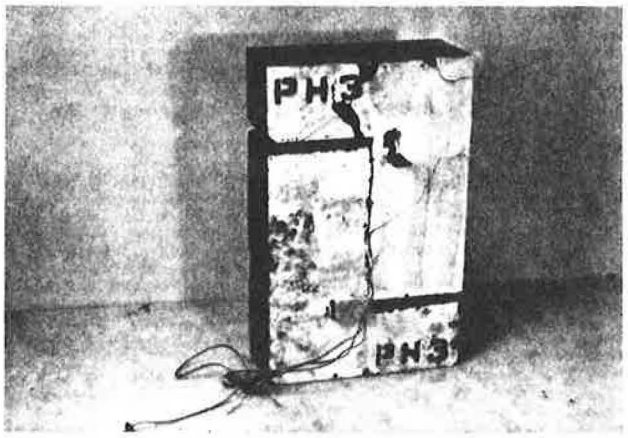

FIGURE 9 Typical failure of PM and PH specimens (spalling of magnesium phosphate concrete).

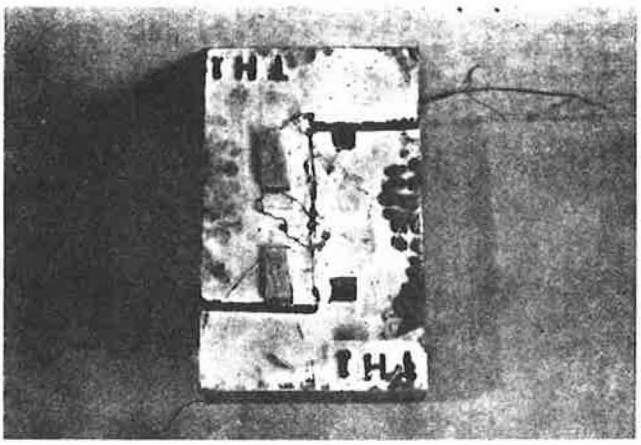

FIGURE 10 Typical failure of TM and TH specimens (spalling of regular concrete).

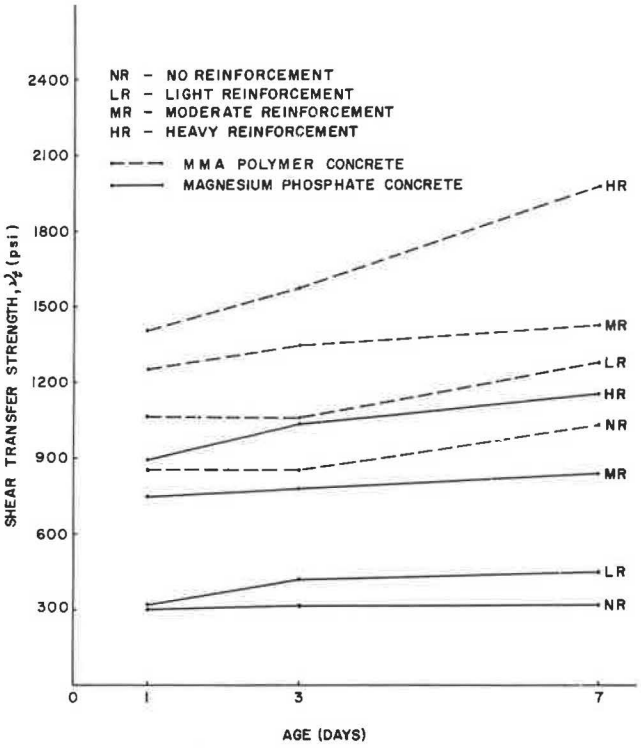

FIGURE 11 Effect of age on shear transfer strength for cold concretes with and without shear reinforcement.

is attained in both the magnesium phosphate and polymer concretes, as shown by the increasing slopes of the plots in Figure 10. This is a result of the increased dowel action contribution to the shear strength at the respective age levels. The 3-day cured specimens illustrate the behavior of the materials at an intermediate time between 1 and 7 days. Therefore, a limited number of specimens were tested at 3 days of age (Tables 1 and 2).

Effect of Shear Reinforcement

The effect of shear reinforcement on shear transfer strength is shown in Figure 12. The slopes of the shear reinforcing

TABLE 1 PUSH-OFF SPECIMEN TEST RESULTS FOR MAGNESIUM PHOSPHATE CONCRETE SPECIMENS

Specimen Identification Code	Shear Reinforcing Strength (psi)	Shear Transfer Capacity (psi)	Number of Test Specimens	Failure Mode
PN1	-	303	2	vertical movement along the shear plane
PN3	-	313	1	
PN7	-	321	2	
PL1	258	321	2	same as above with yielding of transverse
PL3	258	429	1	steel
PL7	258	446	2	
PM1	644	750	2	light diagonal cracking, vertical movement along
PM3	644	786	1	the shear plane, light spalling of magnesium
PM7	644	839	2	phosphate concrete plus steel yield
PH1	965	893	2	light diag. cracking, vert. movement along
PH3	965	1036	1	the shear plane, moderate spalling of magnes-
PH7	965	1143	2	ium phosphate concrete plus steel yield

Notations:

P = Magnesium Phosphate concrete

N = Specimens without any transverse shear reinforcement

L,M,H = Specimens with light, moderate and heavy transverse shear reinforcement respectively

1,2,3 = Specimens cured for 1, 3 and 7 days respectively at 15-20^0 F.

index versus transfer strength line plotted for magnesium phosphate concrete specimens at different ages are almost flat up to a shear reinforcing index of 250 psi. Thus, to take advantage of the dowel action contribution to shear transfer strength of the magnesium phosphate concrete, a minimum shear reinforcing index of 250 psi has to be used. Polymer concrete specimens, on the other hand, appear to gain in strength progressively from the onset of loading.

Figure 10 also gives a plot of the relationship between shear reinforcing index and transfer strength of the control specimens. These specimens represent monolithic construction without cold joints in contrast with the magnesium phosphate and the polymer concrete specimens. Hence, as was expected, shear transfer strength of the control specimens exceeded that of the test specimens by 1,125 percent for magnesium phosphate concrete specimens and 322 percent for polymer concrete specimens due to the monolithic structure of the total control specimen cross section.

Load Deformation Behavior (Slip and Crack Width)

Nonreinforced Specimens

Most related research reports that failure of *nonreinforced* push-off specimens with cold jointed shear plane surfaces is not accompanied by much slip. In this investigation, however, LVDT readings for both the magnesium phosphate and polymer nonreinforced concrete specimens did measure finite slips. Results are presented in Figure 13 for magnesium phosphate concrete and polymer concrete specimens. The variations of slip with applied shear stress are linear up to ultimate loads, at which point the specimens encountered sudden failure. The ultimate slip at 7 days (0.00144 in. at 321 psi stress) for magnesium phosphate concrete is almost twice its slip value at 24 hr (0.000848 in. at 303 psi stress). The magnesium phosphate concrete appears to become more ductile with age. Whereas the variation of slip for polymer concrete specimens with age

TABLE 2 PUSH-OFF SPECIMEN TEST RESULTS FOR MMA POLYMER CONCRETE SPECIMENS

Specimen Identification Code	Shear Reinforcing Strength (psi)	Shear Transfer Capacity (psi)	Number of Test Specimens	Failure Mode
TN1	-	857	2	vertical slip along the shear plane
TN3	-	857	1	
TN7	-	1036	2	
TL1	258	1071	2	same as above with yielding of steel
TL3	258	1071	1	
TL7	258	1286	2	
TM1	644	1250	2	light diagonal tension cracking accompanied
TM3	644	1357	1	by regular concrete spalling plus yielding
TM7	644	1429	2	of steel
TH1	965	1393	2	light diag. tension cracking accompanied
TH3	965	1571	1	by regular concrete spalling plus yielding
TH7	965	1964	2	of steel

Notations: *T = Methyl methacrylate based polymer concrete*

N = Specimens without any transverse shear reinforcement

L,M,H = Specimens with light, moderate and heavy transverse shear reinforcement respectively

1,2,3 = Specimens cured for 1, 3 and 7 days respectively at 15-20^0 F.

TABLE 3 PUSH-OFF SPECIMEN TEST RESULTS FOR CONTROL SPECIMENS

Specimen Identification Code	Shear Reinforcing Strength (psi)	Shear Transfer Capacity (psi)	Number of Test Specimens	Failure Mode
CN	-	1536	2	light to heavy diag. tension cracking, w/concrete
CL	258	1571	2	compression spalling, typical shear failure, plus
CM	644	1964	2	yielding of steel in CL, CM & CH specimens
CH	965	2286	2	

Notations: *C = Control specimens*

N = Specimens without any transverse shear reinforcement

L,M,H = Specimens with light, moderate and heavy transverse shear reinforcement respectively

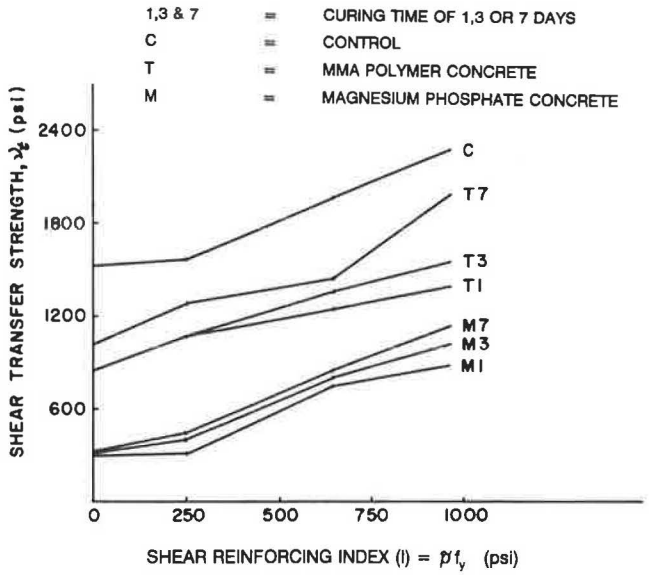

FIGURE 12 Effect of shear reinforcement on shear transfer strength.

was relatively insignificant, indicating that polymer concrete specimens do not exhibit noticeable change in deformation behavior after 24 hr, most of the shear transfer strength contribution for these nonreinforced specimens comes from bond, namely, cohesive strength resulting from high adhesion to the precast concrete. Also, the slip of magnesium phosphate concrete specimens decreases after 3 days. The ultimate slip values for polymer concrete at 1 and 7 days were 0.00789 in. and 0.00824 in., respectively. This indicates that polymer concrete material is several times more ductile than magnesium phosphate concrete material.

Reinforced Specimens

Typical variations of slip and crack width versus shear stress for reinforced specimens are presented in Figure 14 for magnesium phosphate concrete and Figure 15 for polymer concrete specimens. Only results for moderately reinforced specimens are presented because they are typical of all the reinforced specimens. The reinforced test specimens showed very small values of slip and crack width until the formation of the initial vertical cracks along the shear plane. After the development of this crack, both slip and crack width values increased at a faster rate; however, these specimens were still able to carry additional load until ultimate. Increased ductile behavior was observed for slip and crack width with increase in reinforcement levels. Close examination of the slip and crack width plots (Figures 14 and 15) for reinforced specimens indicates that they are similar in pattern. The reliability of the LVDT and the strain gauge readings thus concur. At ultimate load, the maximum slip and crack width values for magnesium phosphate concrete specimens were 0.0638 in. and 0.0043 in., respectively, and for polymer concrete specimens 0.0743 in. and 0.00329 in., respectively. These values point out the similarity in behavior of the two types of cold weather concretes investigated.

A characteristic common to the reinforced specimens is that the rate of increase in slip and crack width appears to vary inversely with the shear reinforcing index. The higher the shear reinforcing index, the lower is the slip and crack width for a given applied shearing load level. An explanation can be given for such behavior of the reinforced specimens. As a reinforced test specimen is loaded, the transverse reinforcing steel is subjected to tensile stresses resulting in development of compressive stresses in the material of the two halves. As the amount of shear reinforcement increases, the force generated in the steel and the surrounding concrete material increases. This confining force is what is responsible for the reduction in deformation.

Performance Comparison of Magnesium Phosphate and Polymer Concretes

Figure 16 presents a comparison of the early-age gain in strength of the two cold weather concrete types. Both concretes exhibit similar trends in strength gain with an increase in reinforcement. The slope of the dotted envelope on the bar plots in both concretes appears to be the same for all ages. The monolithically cast control specimens with similar percentage of reinforcement exhibit higher strength than both the cold weather concretes because of the homogeneity and absence of planes of weakness that the other specimens have. The polymer concrete specimens appear to be considerably stronger than the magnesium phosphate concrete in transferring shearing stresses.

Correlation of the Derived Theory with Experimental Results

A least squares analysis of the test data resulted in the following values of the constants c' and μ' in the expression for total shear transfer capacity v_t in Equation 15:

Age (days)	*Magnesium Phosphate Concrete*		*MMA Polymer Concrete*	
	c'	μ'	c'	μ'
1	248	0.68	890	0.54
3	279	0.78	869	0.74
7	278	0.88	1,015	0.89

For control specimens, the constants are $c' = 1{,}458$ and $\mu' = 0.817$.

These constants are plotted against experimental values in Figure 17 to check their validity. In Figure 17a theoretical and experimental values for the constant c' (cohesive bond strength) are shown for both types of cold weather concretes. There is good agreement between the theoretical and experimental plots for c'. Figure 17b presents a comparison of theoretical and test results for μ' (apparent coefficient of friction) for both types of cold weather concretes. For polymer concrete, 3-day test results appear to be somewhat variable. This probably resulted from the limited number of tests conducted at the 3-day age level. If the 3-day test results are ignored, the polymer concrete test results agree fairly well with the theoretical values.

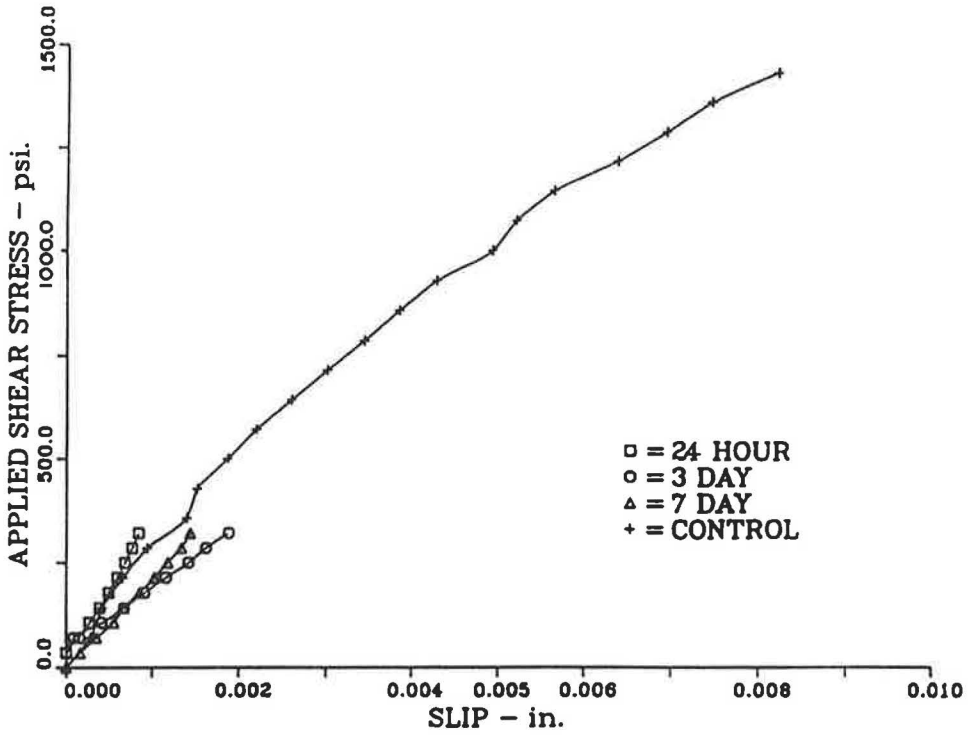

(a) Magnesium Phosphate Concrete Specimens

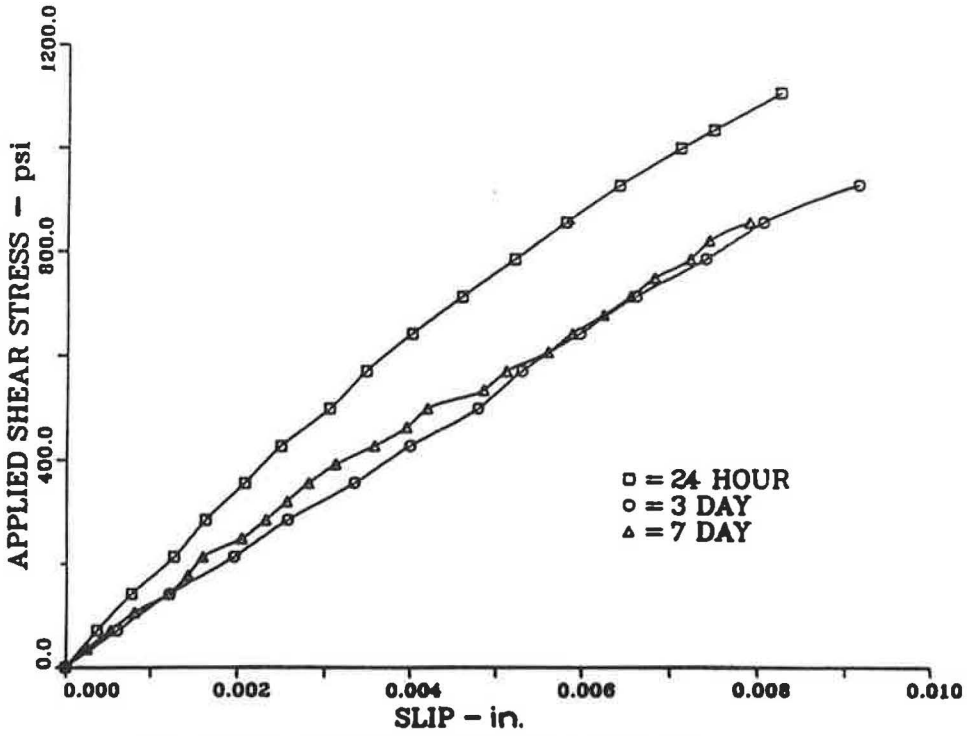

(b) MMA Polymer Concrete Specimens

FIGURE 13 Typical variation of slip with applied shear stress at different ages for nonreinforced specimens.

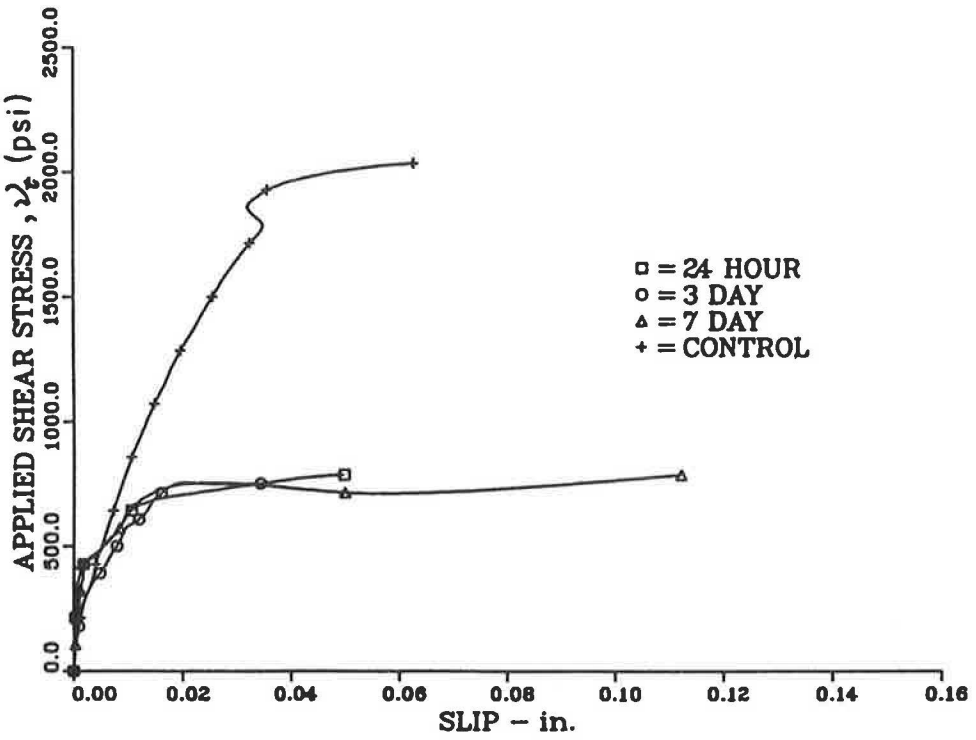

(a) Magnesium Phosphate Concrete Specimens

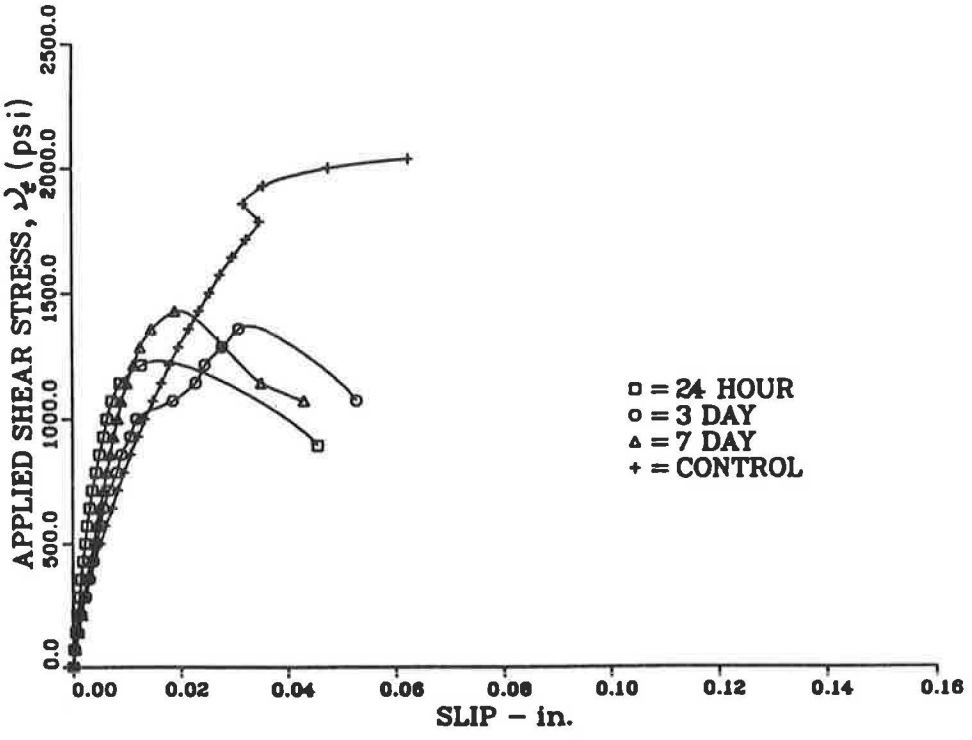

(b) Polymer Concrete Specimens

FIGURE 14 Typical variation of slip with applied shear stress of different ages for moderately reinforced specimens.

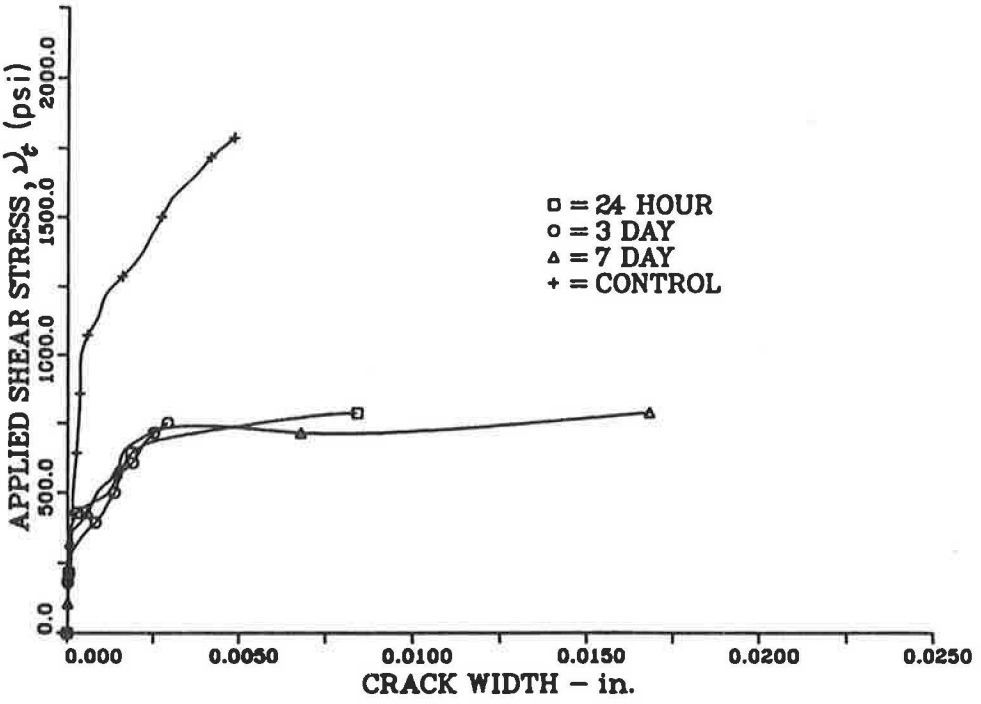

(a) Magnesium Phosphate Concrete Specimens

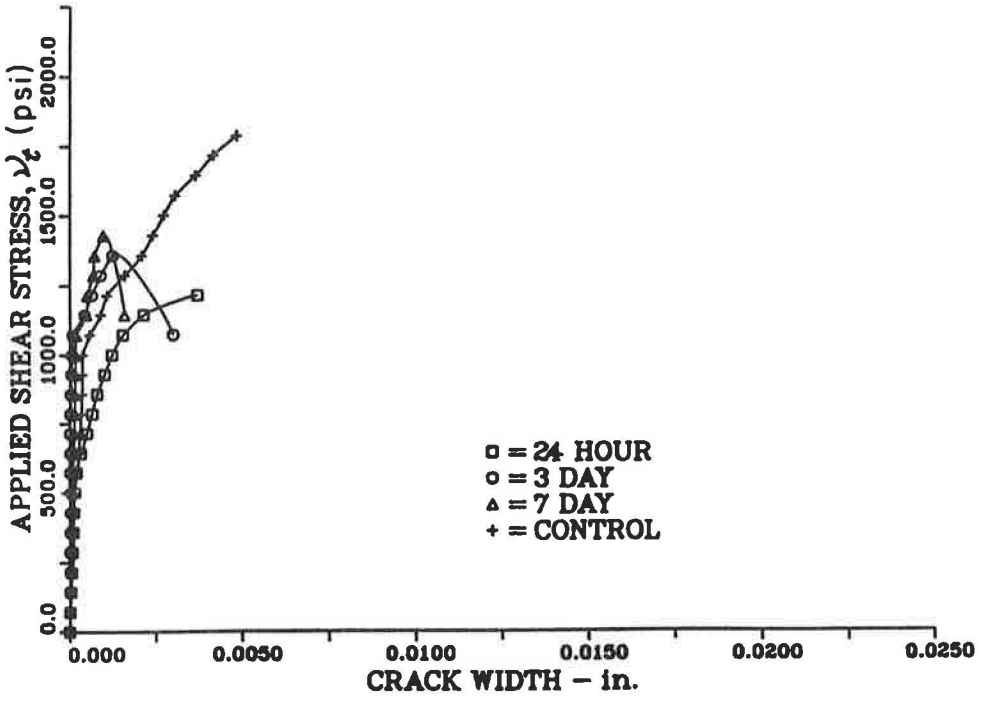

(b) Polymer Concrete Specimens

FIGURE 15 Typical variation of crack width with applied shear stress at different ages for moderately reinforced specimens.

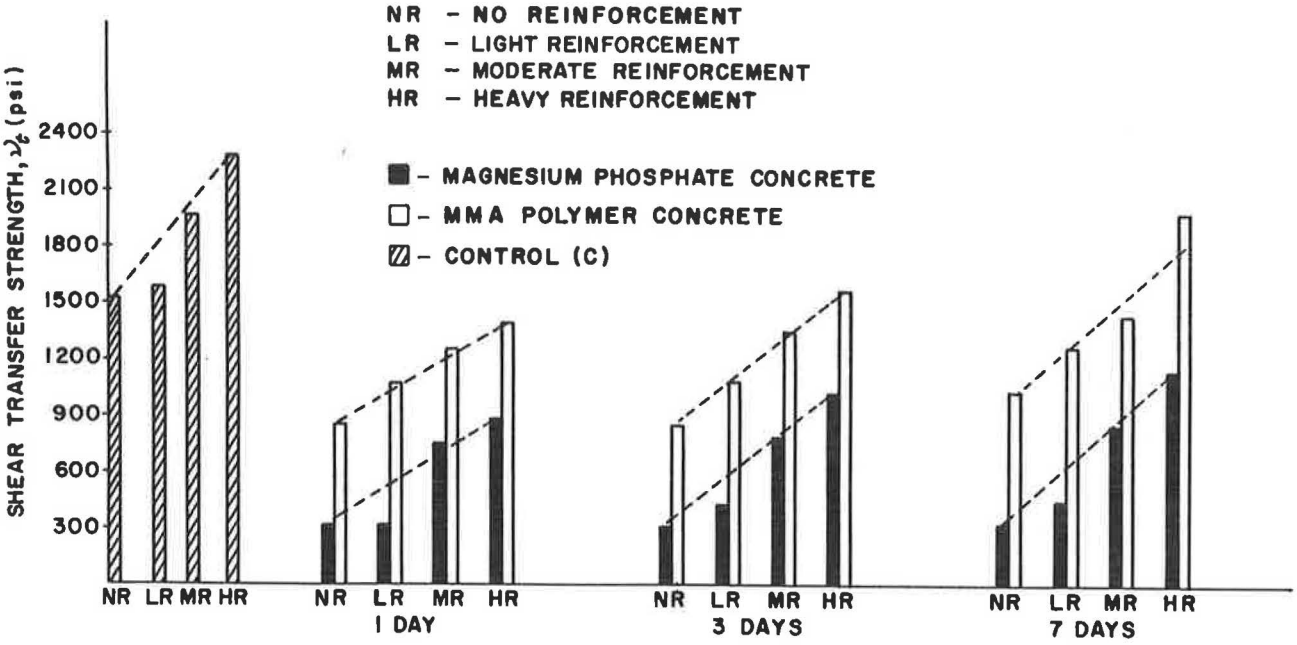

FIGURE 16 Comparison of shear transfer strengths of the cold weather concretes.

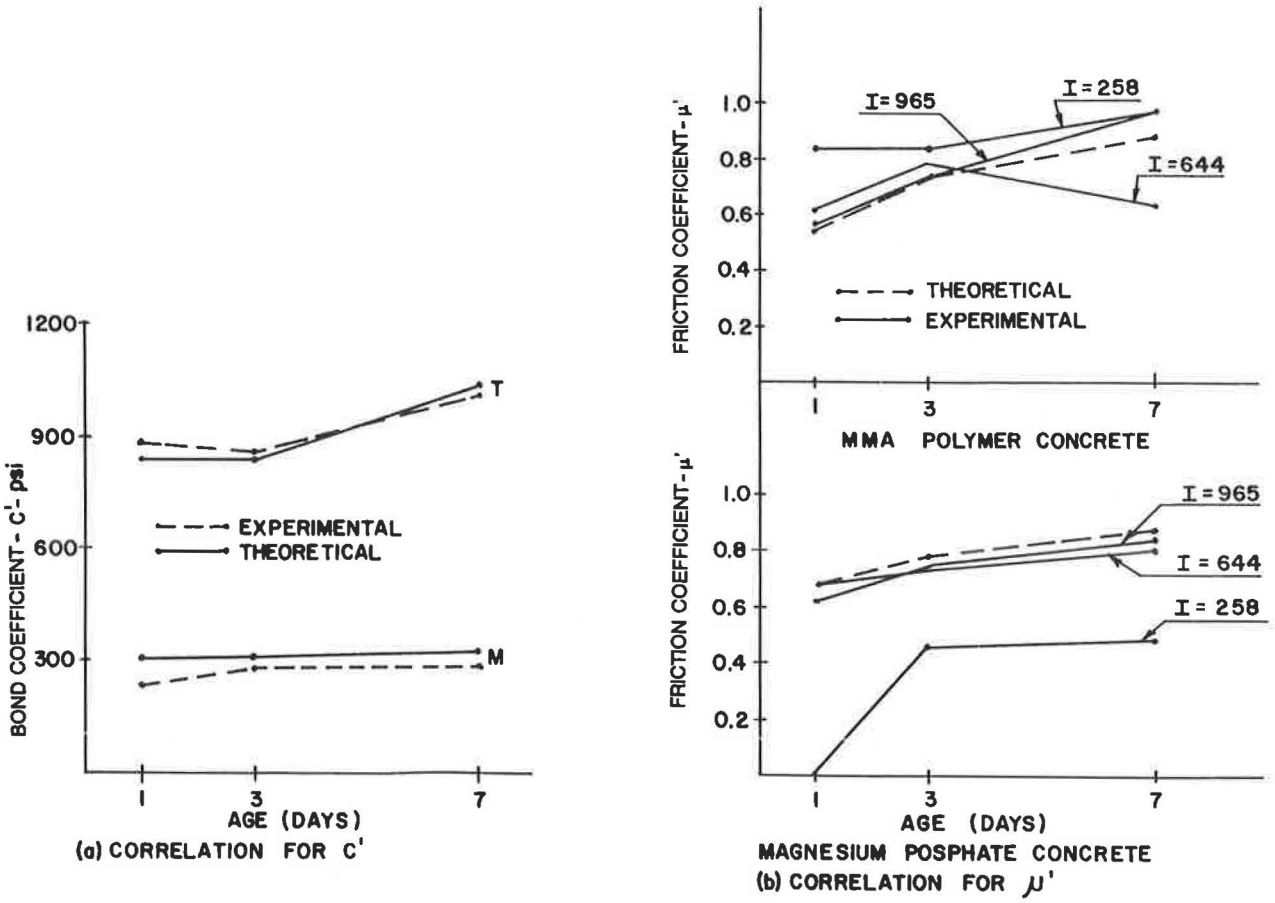

FIGURE 17 Comparison of test results with theoretically derived constants.

Proposed Design Expressions for Shear Transfer Capacity

On the basis of the equation for total shear stress, v_t, Equation 15, $v_t = c' + \mu' I$, and introducing the constants of experiment derived for the two materials and age levels, the following expressions are presented. They are applicable for the design of concrete structural composite sections made of two-layered concretes in subfreezing temperatures having a precast parent regular concrete of strengths up to and exceeding 12,000 psi.

- Magnesium phosphate concrete new layer
  —For early loading conditions based on 1-day test results: $v_t = 248 + 0.68\ I$;
  —For long-term loading conditions based on 7-day test results: $v_t = 277 + 0.88\ I$;
  In the above expressions a minimum of 250 psi for I is recommended.
- MMA polymer concrete new layer
  —For early loading conditions based on 1-day test results: $v_t = 890 + 0.54\ I$;
  —For long-term loading conditions based on 7-day test results: $v_t = 1015 + 0.89\ I$.

Upper Limit for Ultimate Shear Transfer Strength

Because the transverse shear reinforcement becomes very heavy, the theoretical shear resistance due to bond, dowel, friction, and aggregate interlock action becomes greater than the actual shear stress that would cause its failure. The crack in the shear plane locks up in these cases and the behavior and ultimate strength then become the same as that of a monolithically cast specimen. Ultimate shear strength depends on the strength of the weaker of the precast or cold weather concrete material. On the basis of Han-Chin Wu's theory, the upper bound for the ultimate shear transfer capacity is (*11*)

$$v_t = [1.5f'^2_{t2} + 1.426f'_t I - 0.075I^2]^{1/2}$$

where f'_t is the tensile splitting strength of precast or cast in situ concrete, whichever is less.

Because of the material failure of the test specimens at a reinforcement index level of 965 psi, the upper limit for the sum of both components c' and $\mu' I$ can be set at 2,200 psi for polymer concrete and 1,100 psi for magnesium phosphate concrete cast against regular parent concretes of strength up to and in excess of 12,000 psi.

Comparison with ACI Code Provisions for Shear Transfer Strength

Section 11.7 of the ACI Building Code (*17*) lists methods for the design of cross sections subjected to shear transfer at interfaces between dissimilar materials. These provisions allow design for shear transfer based on the shear friction theory proposed by Birkeland and Birkeland (*3*) and Mast (*5*). A comparative study of ACI expression 11.26 for ultimate shear transfer strength, $v_t = 0.85\phi\ \bar{\rho} f_y \mu$ ($\mu = 0.6$ to 1.4) with the experimental results is presented in Figure 18 for both the

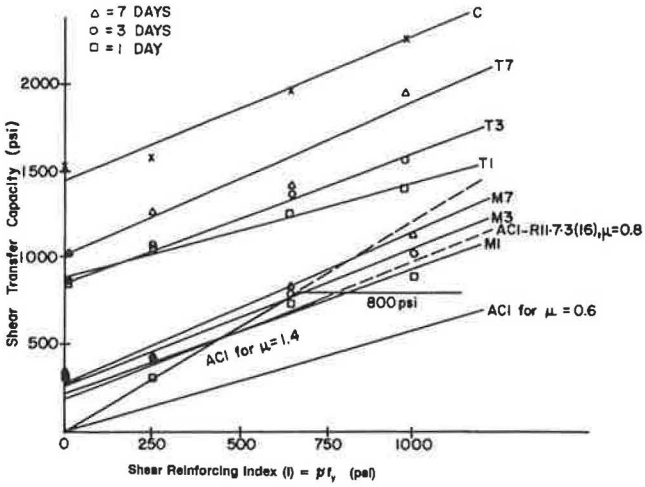

FIGURE 18 Shear transfer capacity versus shear reinforcing strength of magnesium phosphate concrete and MMA polymer concrete and comparison with ACI values.

cold jointed surfaces of cold weather concretes ($\mu = 0.6$) in test specimens and monolithically cast regular concretes ($\mu = 1.4$) in control specimens. In this expression 0.85 is the shear strength reduction factor. Also presented in this figure is the comparison of the test results with the ACI Commentary equation (1b) under section R11.7.3, $v_t = 0.85\ (0.8\ A_s f_y + bdK_1)$, where 0.8 is the coefficient of friction, 0.85 is the shear strength reduction factor, and $K_1 = 400$ psi for normal concrete.

Shear transfer strengths predicted by ACI Equation 11.26 are initially conservative at both the early and late ages for both types of cold weather concretes. This is because the ACI formulations disregard the contribution of apparent cohesive shear transfer strength. At higher values of shear reinforcing strength, the ACI values are in good agreement at all ages of magnesium phosphate concrete, but are conservative for polymer concretes. The control concrete specimens cast under normal weather conditions developed stresses much higher than the two ACI expressions. From the above discussion, it is very clear that MMA polymer concrete can develop shear stresses just by shear and bond in excess of the ACI upper limit of 800 psi even at early ages, whereas the magnesium phosphate concrete can develop the same at early ages with shear reinforcement strengths of 700 psi and greater.

The comparison also validates the previous findings by Nawy and Ukadike (*9*) that the ACI code underestimates the shear transfer strength for polymer concrete layered systems cast under normal weather conditions.

CONCLUSIONS

1. This experimental investigation has identified two types of high-strength cold weather concretes suitable for repairing early-age structural components in subfreezing temperatures and subjected to shearing loads. The two types of concretes are (a) magnesium phosphate concrete (water activated) and (b) MMA polymer concrete. The shear transfer capacity in such concrete elements can be expressed as $v_t = I\mu' + c'$. For a composite element of magnesium phosphate concrete

or polymer concrete cast at subfreezing temperatures against a 12,000-psi conventional precast concrete, the following constants are proposed:

	Magnesium Phosphate Concrete		*MMA Polymer Concrete*	
	c'	μ'	c'	μ'
After 24 hr	248	0.68	890	0.54
After 7 days	278	0.88	890	0.89

Maximum shear transfer capacity for polymer concrete can be taken as 2,200 psi and for magnesium phosphate concrete as 1,100 psi with the parent concrete strength of 1,200 psi or more.

2. At an early age of 24 hr, shear transfer strength of 900 psi and 1,400 psi can be obtained for magnesium phosphate and polymer concretes, respectively, with a reinforcing index of 965 psi.

3. A minimum shear reinforcing index of 250 psi is recommended for magnesium phosphate concrete to take advantage of the contribution of shear reinforcement to shear transfer strength.

4. Both types of cold weather concretes display essentially similar behavior in controlling shear displacements (slip and crack width) at varying ages and transverse reinforcement. The nonreinforced polymer concrete specimens are about five times more ductile than magnesium phosphate concrete specimens with no reinforcement. The pattern of displacements is comparable with that of monolithically cast regular concrete specimens.

5. The changes in slip and crack width vary inversely with the shear reinforcing index.

6. Comparison of the derived expressions and constants from the experimental investigation with the section 11.7 of the ACI building code provisions for ultimate shear transfer strength validates the previous findings by Nawy and Ukadike (*9*) on polymer concretes. ACI underestimates the shear transfer strength at early ages, even for cold weather concretes. Shear stresses in excess of the ACI upper limit of 800 psi can be developed even at early ages with appropriate concrete strengths and reinforcement by cold weather concretes.

ACKNOWLEDGMENTS

The authors wish to acknowledge the support of the FHWA and New Jersey Department of Transportation in funding the initial phase of the project. This work was done by the first author under the direction of the second author in partial fulfillment of requirements for a Ph.D. This project was conducted at the Concrete Research Laboratory of Rutgers, The State University of New Jersey.

REFERENCES

1. E. G. Nawy, A. Hanaor, P. N. Balaguru, and S. Kudlapur. Early Strength of Concrete Patching Materials at Low Temperatures. In *Transportation Research Record 1110*, TRB, National Research Council, Washington, D.C., 1987, pp. 24–33.
2. S. Kudlapur, A. Hanaor, P. N. Balaguru, and E. G. Nawy. *Repair of Bridge Deck Structures in Cold Weather*. Final Report. Department of Civil Engineering, College of Engineering, Rutgers University, Piscataway; N.J. Department of Transportation, Trenton, Aug. 1987, 218 pp.
3. P. W. Birkeland and H. W. Birkeland. Connections in Precast Concrete Construction. *ACI Journal*, Vol. 63, No. 3, March 1966, pp. 345–368.
4. B. Bresler and K. S. Pister. Strength of Concrete Under Combined Stresses. *ACI Journal*, Vol. 55, No. 9, Sept. 1958, pp. 321–345.
5. R. F. Mast. Auxiliary Reinforcement in Precast Concrete Connections. *Proceedings of the American Society of Civil Engineers*, Vol. 94, No. ST6, June 1968, pp. 1485–1504.
6. A. H. Mattock. Design Proposals for Reinforced Concrete Corbels. *Prestressed Concrete Institute Journal*, Vol. 21, No. 3, May-June 1976, pp. 2–26.
7. A. H. Mattock and N. M. Hawkins. Shear Transfer in Reinforced Concrete—Recent Research. *Prestressed Concrete Institute Journal*, Vol. 17, No. 2, March-April 1972, pp. 55–75.
8. T. Paulay and P. J. Loeber. Shear Transfer by Aggregate Interlock. In *ACI Publication SP-42: Shear in Reinforced Concrete*, American Concrete Institute, Detroit, Mich., 1974, pp. 129–166.
9. E. G. Nawy and M. M. Ukadike. Shear Transformation in Concrete and Polymer Modified Concrete Members Subjected to Shearing Loads. *Journal of Testing and Evaluation*, Vol. 11, No. 2, March 1983, pp. 89–98.
10. E. G. Nawy, M. M. Ukadike, and J. Sauer. High Strength Field Polymer Modified Concrete. *Journal of the Structural Division*, ASCE Vol. 103, No. ST-12, Dec. 1977, pp. 2307–2322.
11. M. M. Ukadike. *Durability, Strength and Shear Transfer Characteristics of Polymer Modified Concretes for Concrete Structural Systems*. Ph.D thesis. Rutgers University, Piscataway, N.J., 1978, pp. 132–150.
12. N. C. Palle and T. P. H. Nielsen. Modal Determination of the Effect of Bond Between Coarse Aggregate and Mortar on the Compressive Strength of Concrete. *ACI Journal*, Vol. 66, No. 1, Jan. 1969, pp. 69–72.
13. J. A. Hofbeck, I. A. Ibrahim, and A. H. Mattock. Shear Transfer in Reinforced Concrete. *ACI Journal*, Vol. 66, No. 2, Feb. 1969, pp. 119–128.
14. S. D. Poli, P. G. Gambarova, and C. Karakoc. Aggregate Interlock Role in R. C. Thin-Webbed Beams in Shear. *Journal of the Structural Division*, ASCE, Vol. 113, No. ST-1, Jan. 1987, pp. 1–17.
15. H. Dulacska. Dowel Action of Reinforcement Crossing Cracks in Concrete. *ACI Journal*, Vol. 69, No. 12, Dec. 1972, pp. 754–757.
16. B. R. Hermanson and J. Cowan. Modified Shear Friction Theory for Bracket Design. *ACI Journal*, Vol. 71, No. 2, Feb. 1974, pp. 55–57.
17. *Building Code Requirements for Reinforced Concrete and Commentary—ACI 318R-89*. American Concrete Institute, Detroit, Mich., Nov. 1989, 353 pp.

Publication of this paper sponsored by Committee on Mechanical Properties of Concrete.